Proceedings of the 2005 IEEE
International Conference on Robotics and Automation
Barcelona, Spain, April 2005

Significance of Causality Analysis for Transparent Teleoperation

Hyung-Soon Park
Sensory Motor Performance Program
Rehabilitation Institute of Chicago
345 E. Superior St., Chicago, IL 60611, USA
h-park4@northwestern.edu

Pyung Hun Chang and Jong Hyun Kim
Department of Mechanical Engineering
Korea Advanced Institute of Science and Technology
373-1 Guseong-Dong, Yuseong-Gu, Daejeon, Korea
iskylark@mecha.kaist.ac.kr

***Abstract* – This paper presents significance of causality analysis in attaining transparency of bilateral teleoperation. The causality analysis enabled novel understanding of teleoperation systems, thereby providing methods for finding transparency-attainable control architectures with proper control parameters. Furthermore, when combined with the causality-based stability, stability could still be guaranteed while attaining transparency. Experimental verification is given for simple 1-DOF teleoperation tasks.**

Index Terms* – *Bilateral Teleoperation, Transparency, Causality, Control Architecture.

I. INTRODUCTION

This paper deals with a relatively unnoticed yet very important issue associated with teleoperation systems: ***causality***. In particular, we are going to *present causality analysis on the transparency of teleoperation systems*. Provided below are the context and background for our research on the causality issue.

In general, causality means the cause and effect which has been widely considered in philosophy, jury's prudence, and natural science. In particular, this paper concerns the causality in physical systems: the dependency relationship among system variables that describe the system.

The causality in haptic simulation systems [1] and telemanipulation systems [2] was briefly considered; however, the significance of causality analysis in teleoperation has not been recognized yet. In addition to the recent report on the importance of causality in stability of teleoperation systems [3], this paper presents the significance of causality analysis for attaining transparency. Undoubtedly, the causality analysis will provide us novel understanding of teleoperation system by clarifying the causality among interrelated subsystems: operator, master, slave and environment.

The transparency in teleoperation has been considered as the ideal situation where the human operator feels as if he or she is directly manipulating the remote environment [4]; therefore, the transparency has been used as a performance measure.

Previous literature has shown transparency-attainability of various control architectures (CA's) in relation to the stability issue. Lawrence commented that only the four-channel CA could achieve transparency [5], and H-Zaad stated that two three-channel CA's can also achieve transparency by adding local force feedback loops at the master and the slave [6]; therefore, transparency is attainable only in a few CA's so far—two among four three-channel CA's and the only four-channel CA. In addition to the restricted number of transparency-attainable CA's, when the stability issue is considered, it is difficult to attain transparency since enhancing transparency compromises stability even in teleoperation systems with small communication time delays [5].

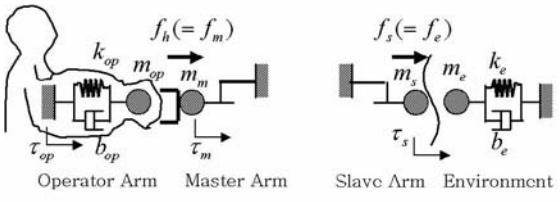

Fig. 1. A one-DOF teleoperation model [8]

To solve those difficulties, this paper adopts causality-based methods. In particular, the objectives of this paper are as follows: 1) to show that transparency is attainable in CA's other than those CA's mentioned in previous works, and 2) to show that transparency is achievable without losing causality-based stability [3].

For causality analysis, we adopted the bond-graph modeling [7] which is known as a good tool for analysing causality.

II. PRELIMINARIES FOR CAUSALITY ANALYSIS

A. Causality in Teleoperation

For simplified analysis, a single-DOF teleoperation model (Fig. 1) is considered.

In Fig. 1, m_{op}, m_m, m_s, and m_e represent masses of the operator, the master arm, the slave arm, and the environment, respectively. Similarly, b_* and k_* denote correspondent damping and stiffness. In addition, v_h, v_m, v_s, and v_e represent velocities of the operator hand, master arm, slave arm, and environment, respectively. Similarly, f_* denotes the corresponding force. τ_{op} represents for the force coming from the operator's muscle while τ_m and τ_s represent for the control forces at the actuators of the master and slave, respectively.

Using the causality assignment procedures in bond-graph modeling [9], two types of causality can be assigned for each of the operator-master part and the slave-environment part.

For the slave-environment part at which the tasks are carried out, task causality is defined by the dependency relationship among the position variables (v_s and v_e) and the force variables (f_s and f_e) in the slave-environment model. The bond-graph for the slave-environment model shows two types of task causality. For Position Commanded Task (PCT) in Fig. 2(a), the position variable ($v_e = v_s$) is

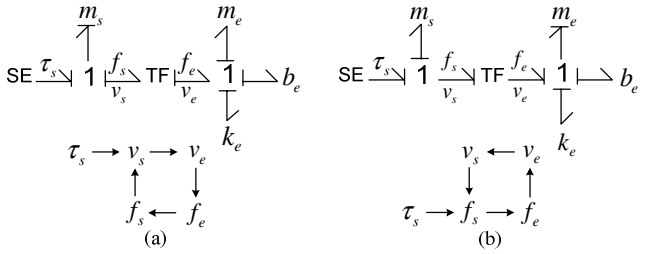

Fig. 2. Task causality: (a) PCT and (b) FCT. Upper figures show the causality assignment using bond-graph. In the bond-graph models, causal strokes (short vertical lines on one end of half arrows) indicate the direction in which the force is directed [7]. Figures below represent the corresponding causality diagram using causality arrows. The causality arrows clearly represent the dependency relationship between two variables. The variable at the end of the arrow is dependent on the variable at the beginning of the arrow.

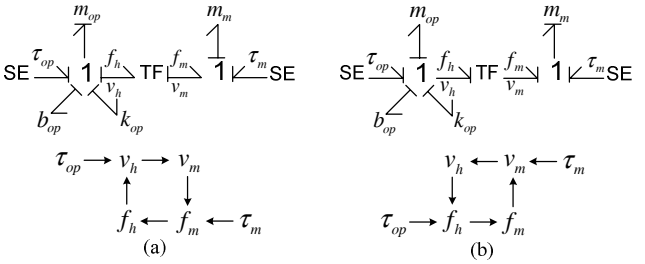

Fig. 3. Operator causality: (a) operator performing PCT, and (b) FCT

independently given to the environment, and the force ($f_s = f_e$) is dependent on the position. On the other hand for Force Commanded Task (FCT), the causality is reversed so that f_e (= f_s) is independently given to the environment, and v_s (= v_e) depends on the force (Fig. 2(b)). For example, positioning tasks such as a free space movement belong to PCT whereas force-applying tasks such as cutting, deburring, and grasping belong to FCT.

Similarly, operator causality is defined by the dependency relationship among the position variables (v_h and v_m) and force variables (f_h and f_m) in the operator-master model.

Two types of operator causality are obtained from the bond-graph of the operator-master model as shown in Fig.3. When the operator is performing PCT, the position of the operator (v_h) is independently determined and the force (f_h) is determined depending on the position (Fig.3(a)). On the other hand, when the operator performs FCT, the force is given independently and the position depends on the force (Fig.3(b)).

From the two types of causality in each of the operator-master and the slave-environment models, four combinations of causality can be found in the teleoperation model as shown in Table I.

B. Control Architectures

The control architectures (CA's) in teleoperation are categorized by the number of communication channels they use and by the types of commands the master and the slave send and receive. Accordingly, nine CA's can be found as listed in Table II.

C. Causality-Based Stability [3]

The causality-based stability analysis proposed causality-consistent control architectures as summarized in

TABLE I. FOUR COMBINATIONS OF CAUSALITY IN TELEOPERATION

	Operator Causality	Task Causality
1	Operator Performing PCT	PCT
2	Operator Performing PCT	FCT
3	Operator Performing FCT	PCT
4	Operator Performing FCT	FCT

TABLE II. CATEGORIZATION OF CONTROL ARCHITECTURES

CA		Master to Slave	Slave to Master
Two-Channel	P-P	Position	Position
	P-F	Force	Position
	F-P	Position	Force
	F-F	Force	Force
Three-Channel	PF-P	Position	Position/Force
	PF-F	Force	Position/Force
	P-PF	Position/Force	Position
	F-PF	Position/Force	Force
Four-Channel	PF-PF	Position/Force	Position/Force

TABLE III. CAUSALITY-CONSISTENT CA'S FOR STABILITY

Operator Causality	Task Causality	Causality-Consistent CA
PCT	PCT	2ch. F-P, P-P
	FCT	3ch. PF-P
FCT	PCT	2ch. F-F, 2ch. P-F
	FCT	3ch. PF-F

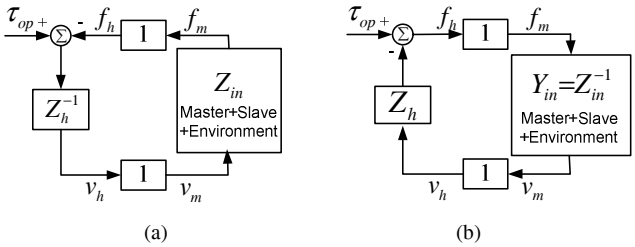

Fig. 4. Two models for causality-based stability: (a) operator performing PCT and (b) operator performing FCT, where Z_{in} and Y_{in} represent overall input impedance and input admittance respectively.

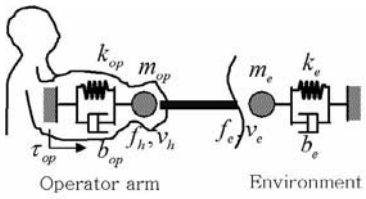

Fig. 5. A one-DOF model for transparency

Table III which brought benefits in designing stable teleoperation systems. By showing that the passivity-based stability methods [2][10][11] guarantee the stability for both of the PCT and FCT which never happen simultaneously, the causality-based stability considers the two cases of causality separately (Fig. 4) in order to obtain stability region larger than the passivity-based stability. Furthermore, the causality-based stability provided easiness in finding control parameters since the stability of input impedance block (Z_{in}) or input admittance block (Y_{in}) could be guaranteed by the local controller of the master and the slave.

III. CAUSALITY-BASED TRANSPARENCY

A. Causality of Transparency Model

A simple one-DOF model of transparency is described in Fig. 5. For the transparency model, two types of causality can also be found by using bond-graph modeling shown in Fig. 6.

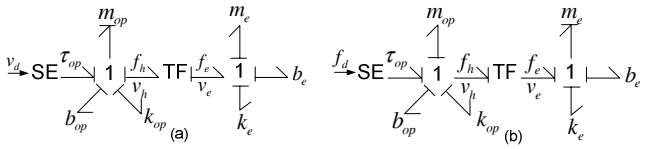

Fig. 6. Two types of causality in the transparency model: (a) In PCT, the operator independently determines the velocity (v_h) by following the virtual velocity trajectory (v_d), and accordingly receives dependent force ($f_h = f_e$) from the environment. (b) In FCT, the operator independently determines the force by following the virtual force trajectory (f_d), and receives dependent velocity ($v_h = v_e$).

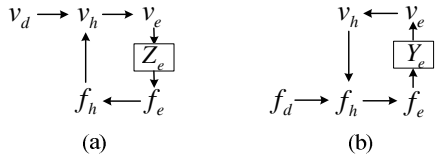

Fig. 7. Causality diagrams of the transparency of (a) PCT, and (b) of FCT

It should be noted that any task must belong to one of the two types, but cannot take both PCT and FCT simultaneously. Therefore, we can separately define the causality-based transparency as the following two.

Definition: Transparency of PCT

Transparency of PCT is the situation where the operator performs PCT directly on the environment (Fig. 7 (a)).

Definition: Transparency of FCT

Transparency of FCT is the situation where the operator performs FCT directly on the environment (Fig. 7 (b)).

For the transparency of PCT, the operator determines v_h as an independent variable and receives dependent force described by

$$f_h = Z_e v_h , \qquad (1)$$

where Z_e represents the impedance of the environment. To implement the transparency of PCT, therefore, the master and the slave should be able to display force described by (1).

On the other hand, for the transparency of FCT, the operator determines f_h as an independent variable and receives dependent velocity described as

$$v_h = Y_e f_h , \qquad (2)$$

where $Y_e = Z_e^{-1}$ represents the admittance of the environment. To simulate the transparency of FCT, the teleoperation devices must be able to display the velocity described by (2)

B. Transparency-Attainable Control Architectures (TACA)

Among the several CA's, TACA will be determined for each of the two types of transparency. In the teleoperation model, it was mentioned that four types of causality exist as listed in Table I. However, in the transparency model, only two types exist; when the operator performs PCT, the position should be independent to the environment; and when the operator performs FCT the force should be independent to the task environment. This implies that the transparency of PCT (or FCT) is not achievable when the operator causality and the task causality are different (case 2 and 3 in Table I). For this reason, to find out transparency-attainable cases, we will deal with the cases when the operator causality and the task causality are same (case 1 and 4 in Table I).

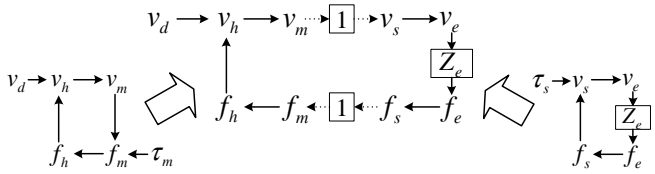

Fig. 8. Desired causality diagram for transparency of PCT

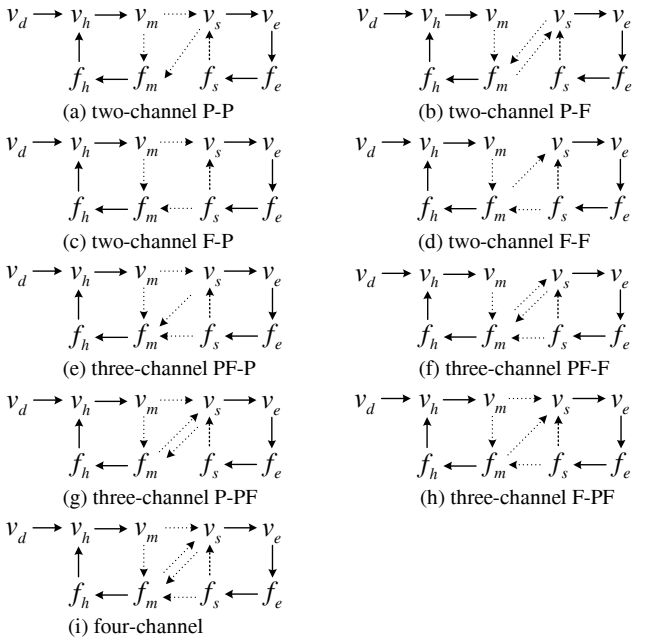

Fig. 9. Causality diagrams for various CA's when both the operator causality and the task causality are PCT.

1) TACA for PCT: In Fig. 8, the desired causality diagram is drawn by slightly modifying the causality diagram of transparent PCT in Fig. 7(a). The desired causality diagram is drawn to involve variables of the master and the slave. Since we consider PCT for both the operator causality and the task causality, v_h is determined independently at the operator-master model resulting in the following causality arrows: $v_h \rightarrow v_m$, $v_m \rightarrow f_m$, $f_m \rightarrow f_h$, and $f_h \rightarrow v_h$ (left hand diagram), while v_s is determined independently at the slave-environment model resulting in the following arrows: $v_s \rightarrow v_e$, $v_e \rightarrow f_e$, $f_e \rightarrow f_s$, and $f_s \rightarrow v_s$ (right hand diagram). If the two diagrams can be combined to result in the diagram at center, the transparency of PCT represented by Fig. 6 (a) (or Fig. 7 (a)) is achieved. In particular, we should be able to cancel $v_m \rightarrow f_m$ and $f_s \rightarrow v_s$, meanwhile we should be able to add arrows from v_m to v_s, and from f_s to f_m with unit gains.

To investigate the transparency-attainability of nine CA's causality diagrams for each CA are drawn. First, for the four two-channel CA's, the causality diagrams are drawn in Fig. 9(a) ~ (d). For example of P-P architecture, we add the arrows, $v_m \rightarrow v_s$ and $v_s \rightarrow f_m$; v_m is sent to the slave to determine v_s whereas v_s is sent back to the master having influences on f_m. Note that the command from the slave has direct influences on f_m since the operator causality is PCT; the operator determines v_m independently so that the commands from the slave can never determine v_m again but have influences on f_m. In the similar ways, we can easily draw the diagrams for P-F, F-P, and F-P architectures.

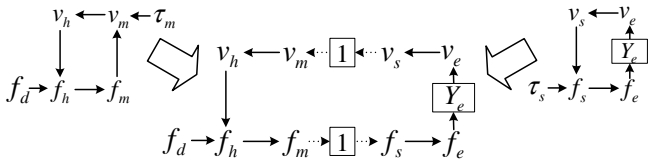

Fig. 10. Desired causality diagram for transparency of FCT

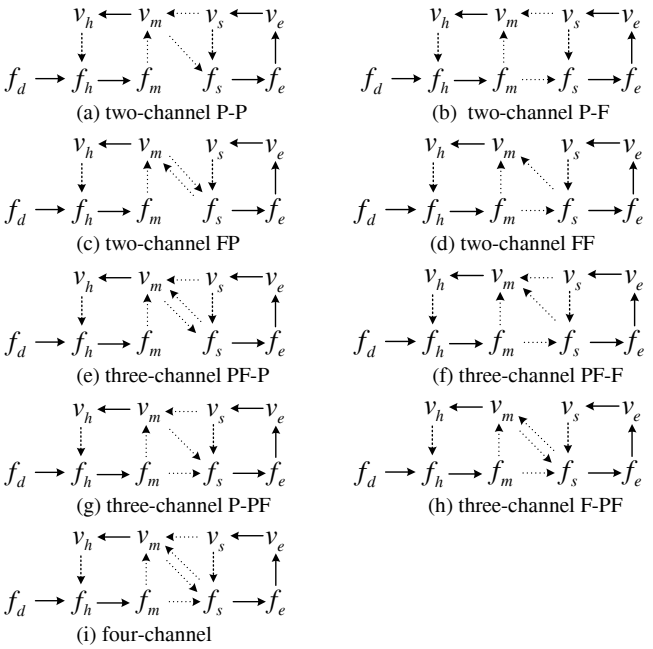

(a) two-channel P-P (b) two-channel P-F (c) two-channel FP (d) two-channel FF (e) three-channel PF-P (f) three-channel PF-F (g) three-channel P-PF (h) three-channel F-PF (i) four-channel

Fig. 11. Causality diagrams for various CA's when both the operator causality and the task causality are FCT.

Given the causality diagrams, we can easily determine the transparency-attainability. F-P architecture can attain transparency whereas the other three two-channel CA's cannot; we can cancel out $v_m \rightarrow f_m$ and $f_s \rightarrow v_s$ by introducing proper control laws; however, we cannot add arrows from v_m to v_s, and from f_s to f_m for P-P, P-F, or F-F architecture. Similarly, the transparency-attainability of three-channel CA's and four-channel CA can be determined from the causality diagrams shown in Fig.9(e)~(h) and Fig.9(i). Among three-channel CA's, transparency is attainable for PF-P and F-PF architectures, and four-channel CA can achieve transparency as was reported in [5].

2) TACA for FCT: TACA for FCT can be found in the similar way. First, the desired causality diagram is drawn (Fig. 10). Using FCT for both the operator causality and the task causality, we can determine the causality arrows for the operator-master part (left hand diagram) and the slave-environment part (right hand diagram). To achieve transparency of FCT (Fig.7(b)), we should be able to cancel out the arrows, $f_m \rightarrow v_m$ and $v_s \rightarrow f_s$, meanwhile we should be able to add arrows from f_m to f_s, and from v_s to v_m to obtain the desired causality diagram.

With the transparency achieved, the velocity felt by the operator is represented by (2).

To find out the TACA for FCT, the causality diagrams for two-channel CA's (Fig.11(a)~(d)), three-channel CA's (Fig.11(e)~(h)), and the four-channel CA (Fig.11(i)) are drawn. Among four two-channel CA's, it is obvious that P-F architecture can achieve the desired causality diagram whereas P-P, F-P, and F-F architectures cannot. Among three-channel CA's, PF-F and P-PF architectures are transparency-attainable while four-channel CA can always attain transparency as mentioned in [5].

In summary, TACA for each of PCT and FCT are listed in Table IV.

TABLE IV. TRANSPARENCY-ATTAINABLE CONTROL ARCHITECTURES

	PCT	FCT
Two-Channel	F-P	P-F
Three-Channel	PF-P, F-PF	PF-F, P-PF
Four-Channel	Always Attainable	

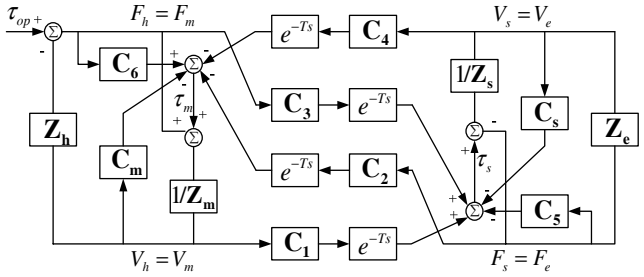

Fig. 12. Generalized representation of teleoperation system [6]

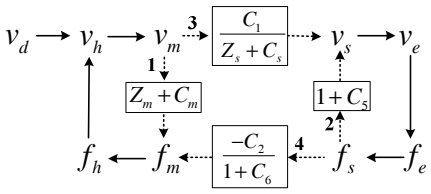

Fig. 13. Example of Finding TACP (Two-Channel F-P)

C. Transparency-Attaining Control Parameters (TACP)

For each TACA summarized in Table IV, control parameters to attain the transparency are found by deriving the gains involved in each of the arrows in the causality diagrams. To derive the gains, the nomenclature of the generalized representation (Fig. 12) is considered.

From the block diagram (Fig. 12) all causality diagrams can be re-drawn in detail with the gains involved in each causality arrow. For example, the causality diagram for the two-channel F-P architecture can be re-drawn like Fig. 13. As aforementioned, the gains involved in arrow 1 and 2 should be equal to zero and the gains involved in arrow 3 and 4 should be equal to unity for transparency. Finally, we can get the following four constraint equations for transparency.

$$C_m = -Z_m \tag{3}$$

$$C_5 = -1 \tag{4}$$

$$C_1 = Z_s + C_s \tag{5}$$

$$C_2 = 1 + C_6 \tag{6}$$

For the other TACA, the constraint equations can be found similarly by re-drawing the causality diagram with gains involved in each arrow, and we can obtain TACP as summarized in Table V.

The TACP for three-channel PF-P, three-channel P-PF, and the four-channel architectures are same with the previously reported transparency-optimizing parameters (TOP)[2][5]. However, the TACP for three-channel F-PF and PF-F are newly proposed in this paper, and TACP for

TABLE V. TRANSPARENCY-ATTAINING CONTROL PARAMETERS FOR TACA

	TACA	Transparency-Attaining Control Parameters				
		C_1	C_2	C_3	C_4	Constraints
PCT	F-P	Z_s+C_s	$1+C_6$			$C_5=-1$, $C_m=-Z_m$
	PF-P	Z_s+C_s	$1+C_6$		$-(Z_m+C_m)$	$C_5=-1$
	F-PF	Z_s+C_s	$1+C_6$	$1+C_5$		$C_m=-Z_m$
	4ch.	Z_s+C_s	$1+C_6$	$1+C_5$	$-(Z_m+C_m)$	
FCT	P-F			$1+C_5$	$-(Z_m+C_m)$	$C_6=-1$, $C_s=-Z_s$
	PF-F		$1+C_6$	$1+C_5$	$-(Z_m+C_m)$	$C_s=-Z_s$
	P-PF	Z_s+C_s		$1+C_5$	$-(Z_m+C_m)$	$C_6=-1$
	4ch.	Z_s+C_s	$1+C_6$	$1+C_5$	$-(Z_m+C_m)$	

TABLE VI. SUMMARY OF CAUSALITY-CONSISTENT CA'S

Causality		Causality-Consistent CA		
Op.	Task	Stability	Transparency	**Both**
PCT	PCT	2ch. F-P 2ch. P-P 3ch. PF-P	2ch.F-P, 3ch.PF-P, 3ch.F-PF, 4ch.	**2ch. F-P** **3ch. PF-P**
	FCT		N/A	**N/A**
FCT	PCT	2ch. P-F 2ch. F-F 3ch. PF-F	N/A	**N/A**
	FCT		2ch.P-F, 3ch.PF-F, 3ch.P-PF, 4ch.	**2ch. P-F** **3ch. PF-F**

the two-channel architectures achieve more transparent teleoperation than the previous TOP do, which will be shown by experiment in the next section.

D. Transparency with Time Delay

Ideally, the definition of transparency does not include any time delay terms since it describes the operator directly interacting with the environment. In reality, however, the time delay between the master and the slave is inevitable. If the time delay (T) exists between the master and the slave, the unit gains in Fig. 8 should be replaced by e^{-Ts} and the operator felt force changes into

$$f_h = e^{-2Ts} Z_e v_h , \quad (7)$$

which represents delayed transparency of PCT. Similarly, for FCT, the operator felt velocity can be represented by

$$v_h = e^{-2Ts} Z_e^{-1} f_h . \quad (8)$$

The delayed transparency can be felt transparent when the delay remains below the human reaction time (T<50msec) [12]. For larger delays, however, the delayed transparency may cause difficulties showing the need of other performance measures than the transparency. Since this paper deals with the transparency, we focus on teleoperation with small time delays up to 50msec.

E. Relation with the Stability Issue

For successful teleoperation, stability should be guaranteed before attaining transparency. For the stability of teleoperation systems, passivity-based stability methods [2][10][11] were popularly considered. Unfortunately, it trades off the transparency at the cost of attaining stability. In particular, it was reported that the use of TOP lost passivity even for small time delays; therefore, the TOP was applicable only for negligible time delays [2]. The loss of passivity (or absolute stability) does not imply instability; however, there is no guarantee of stability either.

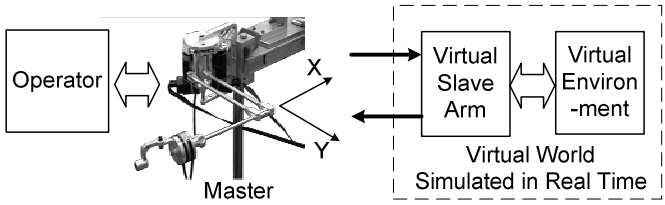

Fig. 14. Experimental setup

To this difficulty, the causality-based stability enables the use of TACP in Table V for small but non-negligible time delays. For example of the two-channel F-P architecture, a condition for absolute stability [2] is written as

$$\eta(\omega) = \cos(\angle e^{-j2\omega T}) + 2\frac{1+C_5}{1+C_6}\Re\{Z_m + C_m\}\Re\left\{\frac{1}{Z_s+C_s}\right\} \geq 1 \text{ for} \forall \omega . \quad (9)$$

With the TACP given in Table V, above condition is never satisfied. Although dissatisfaction of the absolute stability does not mean instability, the stability cannot be guaranteed either. However, by considering causality-based stability and thereby applying the F-P architecture to PCT (refer Table III), the stability is still guaranteed even for the TACP. By using the TACP, Z_{in} in Fig. 4(a) (the case of PCT) is represented as

$$Z_{in} = \frac{D_{Vm}D_{Vs} + e^{-2Ts}C_1C_2Z_e}{(1+C_6)D_{Vs}} , \quad (10)$$

where $D_{Vm} = Z_m + C_m$, and $D_{Vs} = Z_s + C_s + (1+C_5)Z_e$.

The use of TACP does not introduce RHP (right half plane) poles in Z_{in} since poles of D_{Vs} are already placed in LHP (left half plane) when designing local slave feedback control. This example shows the benefits of causality analysis in both of the stability and transparency. For both stability and transparency, the causality-consistent CA's are summarized in Table VI. To satisfy causality-consistency for both stability and transparency, the two-channel FP architecture is adequate for PCT and the two-channel PF architecture is adequate for FCT.

IV. EXPERIMENTS

For verification, simple experiments were performed for one-DOF teleoperation tasks. The operator moved 2-DOF haptic device along the x-coordinate (Fig. 14). The slave contacting with the environment was simulated virtually. All controls for the master and the virtual slave were performed in real-time OS with 200Hz sampling rate with the communication time delay of 50msec.

First, the operator performed a positioning task (PCT) when the slave made contact with a compliant environment. For causality-consistency, two-channel F-P architecture was implemented with two different sets of control parameters; TOP and TACP (Table VII). For stability, since the two-channel F-P is consistent with PCT, both the TOP and TACP could be performed without going unstable (Fig.15) although both of them could not satisfy the absolute stability condition given by (9). For transparency, the position tracking error and the force tracking error are much smaller for TACP, which verified enhanced transparency than the TOP (Fig. 15).

TABLE VII. IMPEDANCE AND CONTROL PARAMETERS USED IN EXPERIMENT

	2ch. F-P for PCT		2ch. P-F for FCT	
	TOP	TACP	TOP	TACP
Z_m	0.04s + 0.01 + 48/s			
Z_s	6s + 10 + 100/s			
Z_e	s + 5 + 50/s (compliant)		s + 5 + 1000/s (stiff)	
C_5	-0.1	-1	0.9	
C_6	0.9		-0.1	-1
C_m	-0.04s -0.005 - 6/s	$-Z_m$	0.01 + 48/s	
C_s	10 + 100/s		-6s - 5 - 50/s	$-Z_s$

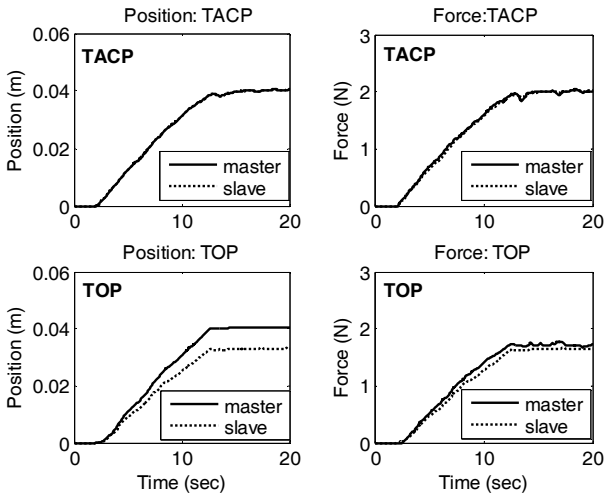

Fig. 15. Experimental results: 2ch. F-P applied for PCT

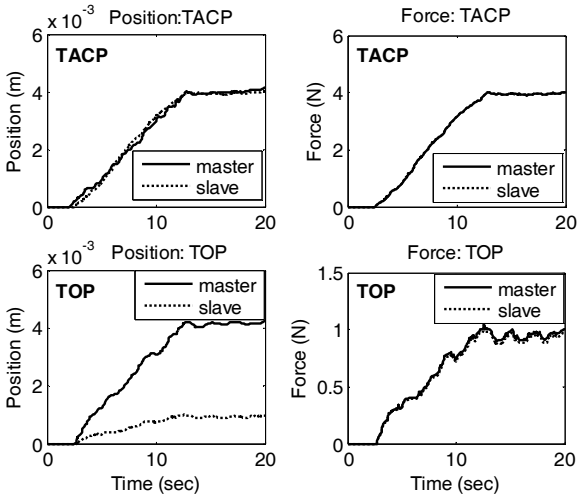

Fig. 16. Experimental results: 2ch. P-F applied for FCT

Second, the operator performed a force applying task (FCT) when the slave made contact with a stiff environment. For causality-consistency, two-channel P-F architecture was implemented with TOP and TACP given in Table VII. Due to the causality-consistency with respect to the stability, the two-channel P-F showed stable operation (Fig.16) even though the two sets of control parameters did not satisfy the absolute stability condition. For transparency, the TACP showed much enhanced transparency than the TOP.

Throughout the experiments, we could confirm 1) the transparency-attainability of the two-channel F-P, and P-F architectures which have not mentioned before, and 2) the stability guaranteed by the causality-based stability.

V. CONCLUSION

The significance of causality analysis is shown for the transparency of teleoperation. From causality analysis on the teleoperation, we could find two types of causality: PCT and FCT. Since the two types never occur simultaneously, we could separately define the transparency of PCT and FCT. This separation brought advantages in two aspects; first, we could suggest more TACA other than the CA's mentioned in previous works; and second, we could achieve transparency with guaranteed stability by incorporating the causality-based stability. The TACP proposed in this paper enhanced transparency compared to the TOP proposed previously.

The benefits of the causality-based approach can be summarized as follows. For negligible time delays, the causality-based transparency additionally provides TACP for two-channel F-P and P-F architectures, and three-channel F-PF and PF-F architectures, thereby providing more choices for the teleoperator design. For small but non-negligible time delays, the causality-based approach enables transparency-achievement with guaranteed stability.

For large time delays, the implementation of transparency defined by (3) or (4) may cause a problem because the delayed feeling induces difficulties for the operator performing the task properly. In the future, the transparency in large time delays should be defined in a different way to make the operator perform the task easily.

REFERENCES

[1] R. Adams and B. Hannaford, "Stable Haptic Interaction with Virtual Environments," *IEEE Trans. Robotics and Automation*, vol.15, no.3, pp. 465-474, 1999.

[2] K. Hashtrudi-Zaad, and S. Salcudean, "Analysis of control architectures for teleoperation systems with impedance/admittance master and slave manipulators," *Int. J. of Robotics Research*, vol. 20, no. 6, pp. 419-445, 2001.

[3] H. Park, and P. Chang, "Causality analysis using bond-graph and its significance in bilateral teleoperation," *Proc. of IEEE/RSJ Int. Conf. on Intelligent Robots and Systems*, pp. 2991-2998, October 2002.

[4] T. Sheridan, "Telerobotics," *Automatica*, vol. 25, no. 2, pp. 487-507, 1989.

[5] D. Lawrence, "Stability and transparency in bilateral teleoperaton," *IEEE Trans. Robotics and Automation*, vol. 9, no. 5, pp. 624-637, 1993.

[6] K. Hashitrudi-Zaad, and S. Salcudean, "On the use of local force feedback for transparent teleoperation," *Proc. of IEEE International Conference on Robotics & Automation*, pp.1863-1869, 1999.

[7] R. Rosenberg, and D. Karnopp, *Introduction to Physical System Dynamics*, McGraw-Hill, 1983.

[8] Y. Yokokohji, and K. Yoshikawa, "Bilateral control of master-slave manipulators for ideal kinesthetic coupling-formulation and experiment," *IEEE Trans. Robotics and Automation*, vol. 10, no. 5, pp. 605-620, 1994.

[9] R. Rosenberg, "Exploiting bond graph causality in physical system models," *ASME J. of Dynamic Systems, Measurement, and Control*, vol. 109, pp. 378-383, 1987.

[10] R. Anderson, and M. Spong, "Bilateral control of teleoperators with time delay," *IEEE Trans. on Automatic Control*, vol. 34, no. 5, pp. 494-501, 1989

[11] G. Neimeyer, and J. Slotine, "Stable Adaptive Teleoperation," *IEEE J. of Oceanic Eng.*, vol. 16, no. 1, pp. 152-162, 1991.

[12] G. Neimeyer, and J. Slotine, "Telemanipulation with Time Delay," *Int. J. of Robotics Research*, vol.23, no. 9, pp.873-890, 2004